

## 10. Attenuation of Shear Waves in Soil.

By Kazuyoshi KUDO and Etsuzo SHIMA,

Earthquake Research Institute.

(Read Nov. 22, 1969.—Received Jan. 24, 1970.)

### 1. Introduction

Since the early days of seismology, many seismologists and earthquake engineers have paid much attention to the mechanism of intrinsic attenuation of waves in the earth materials. The problem is generally discussed in terms of attenuation coefficient or  $Q$ -value. As is well known,  $Q$ -value is proportional to frequency in the model suggested by Maxwell (1867). Such material is referred to as a Maxwell solid. Contrarily, it is inversely proportional to frequency in the model proposed by Meyer (1874a, 1874b), Kelvin (1878) and Voigt (1892). Such material is referred to as a Voigt solid. Many investigators attempted to explain the problem by means of the above mentioned simple models. Iida (1934, 1935, 1938a, 1938b, 1938c), Ishimoto and Iida (1936a, 1936b) investigated the properties of sand, clay and pitch-like materials by means of the vibration method and proposed that they behaved as the Voigt solids. Ricker (1953) studied the breadths and amplitudes of the seismic wavelets in Pierre shale, and explained the shale as the Voigt solid. While, Hirono (1935a, 1935b, 1941), Miyabe and Ooi (1949) attempted to explain the materials by the Maxwell solid. Adopting the Toda's model, Kubotera (1952) obtained the relaxation times, which are intimately related with the attenuation coefficient, associated with the crustal materials and the alluvial deposits using  $P$  waves.

On the other hand, from the laboratory experiment, Born (1941) showed that the attenuation of seismic pulses in the dry samples of earth materials was proportional to frequency, namely  $Q$ -values in such materials were constant. Similar results were obtained by Collins and Lee (1956) associated with the sandstone. McDonal et al (1958) studied the attenuation of compressional and shear waves in the Pierre shale. They found that the attenuation of seismic waves was proportional to frequency. Tullios and Reid (1969) acquired the same results as McDonal et al using  $P$  waves in the Gulf Coast sediments. Knopoff (1956), Knopoff and MacDonald (1958) emphasized that the attenuation is due to the solid friction. If this is the case, the attenuation is proportional to the frequency and no dispersion can exist in body waves.

Horton (1959), Futterman (1962), Wuenschel (1965) and Strick (1967), however, detected the dispersion of body waves from the seismograms obtained by McDonal et al (1958). Furthermore, as is represented by the papers of Lomnitz (1957, 1962), Futterman (1962) and others, there is a stream of thought that the attenuation is approximately proportional to frequency only in the limited frequency range, employing the theory of linear viscoelasticity. Thus, there are two schools of thought in the study of loss mechanism associated with the earth materials. This is mainly due to the fact that our observations are limited to a narrow range of frequency.

As mentioned above, the loss mechanism has not yet been investigated sufficiently, and it still remains as an outstanding problem to be clarified. Although there are many papers associated with the problem, almost all of them are related to the earth crust and mantle. Since the S wave measurement of soil layers in situ was believed to be difficult until quite recently, former investigators studied the attenuation of P waves and only a few papers associated with the S waves have hitherto been published. Nowadays, S wave measurement in situ has become an easy routine work. Therefore, persistent study of the attenuation of S waves measured in situ is necessary, since the study will supply a great deal of information clarifying the loss mechanism and the behavior of soil during earthquakes. In the following, an effort along the above mentioned lines is reported.

## 2. Experiments and Data

Experiments were carried out at four places in the Tokyo Metropolis. They are Adachi, Sunamachi, Yukigaya and Yayoi (Table 1). The natural period and the damping coefficient of the borehole seismometer used in these experiments were 0.2sec and 0.6, respectively. The output voltage of the seismometer was amplified by means of the DC amplifier and then connected to the galvanometer having a natural frequency of 100 cps. Consequently, frequency characteristics of the total system were flat with respect to the ground velocity in the frequency range from 8 to 70 cps.

Table 1.

| No. | Location  | Address of the site                  |
|-----|-----------|--------------------------------------|
| 1   | Adachi    | Motogi-nishi-machi, Adachi-ku, Tokyo |
| 2   | Sunamachi | 5, Kitasuna, Koto-ku, Tokyo          |
| 3   | Yukigaya  | Yukigaya, Ota-ku, Tokyo              |
| 4   | Yayoi     | 1, Yayoi-cho, Bunkyo-ku, Tokyo       |

Fig. 1 shows the method of observation schematically. Seismic waves were generated at the position 1m from the borehole in each experiment by hitting horizontally, with a wooden hammer, the end of a slender weighted wooden plate laid down on the ground surface. Waves thus generated were observed by the borehole seismometer at different depths. The waves detected by the horizontal components, oriented in the same direction with that of the force, were confirmed as SH waves, since the inversion of corresponding phases was noticed when hitting the reverse end of the source plate.

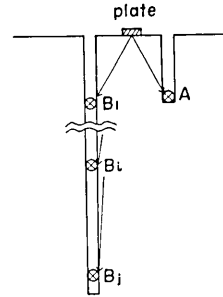


Fig. 1. Configuration of source plate and borehole seismometers. Seismometer at the position A was fixed all through the experiment and the seismometer at the position B was installed at various depths.

Six vertical travel times for SH waves were obtained from independent trials at one depth. Travel times thus obtained were averaged and the amount of times, depth/200 m/s, were reduced. Such reduction is convenient for seeing roughly

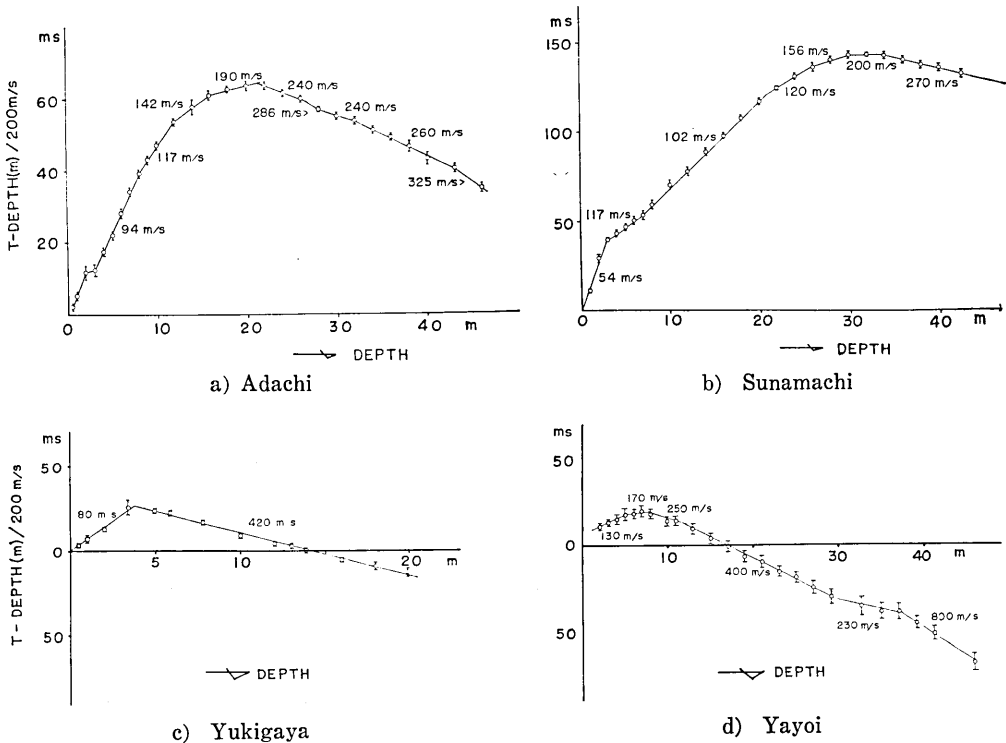
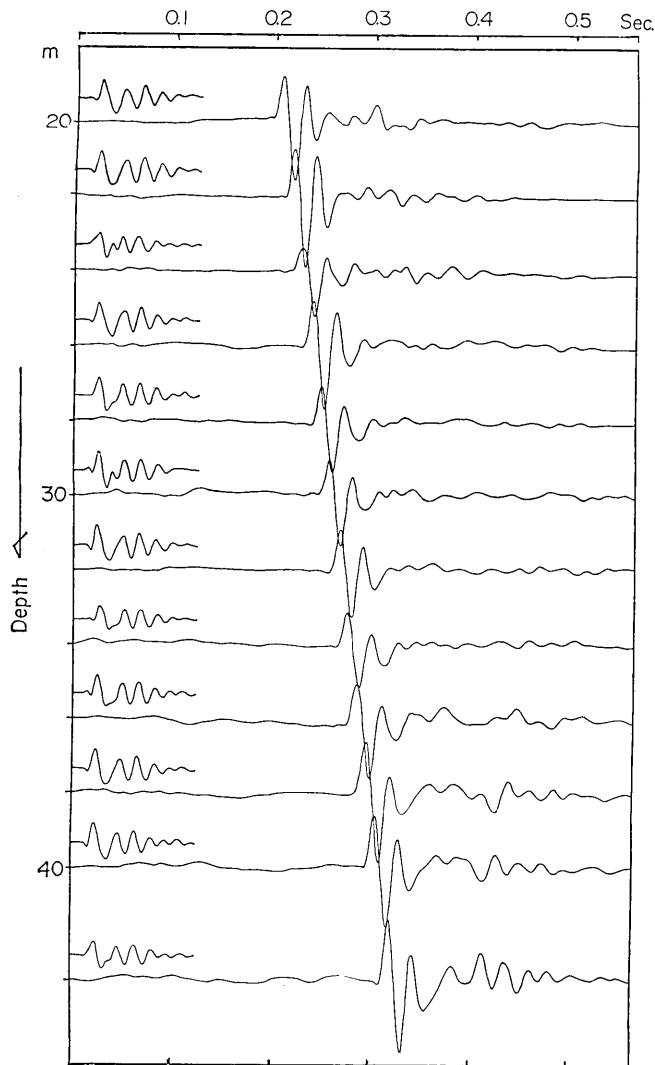


Fig. 2. The reduced vertical travel time graphs for SH-waves. Bars show 95% confidence intervals.



a) Adachi

Fig. 3a. Sample seismograms of vertically travelling SH waves. Shorter ones are reference seismograms obtained at fixed position A.

if the soils are of diluvial or alluvial deposits, since the S wave velocities in alluvial soils are lower than 200 m/s while those in diluvial soils are higher than 200 m/s (Shima et al, 1968). Therefore, one may easily classify the soils into the above mentioned two formations depending upon the gradients of the reduced travel times. Reduced travel times, shown by circles, are shown in Figs. 2a, 2b, 2c and 2d. Confidence intervals of 95% (shown by vertical bars) were also computed and are shown in the figures. From these figures, we found the layers in which the SH wave velocities were fairly uniform. The seismograms observed

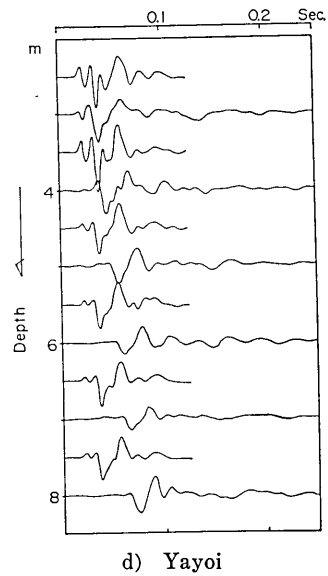
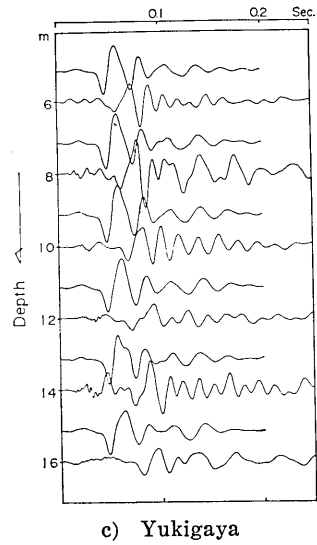
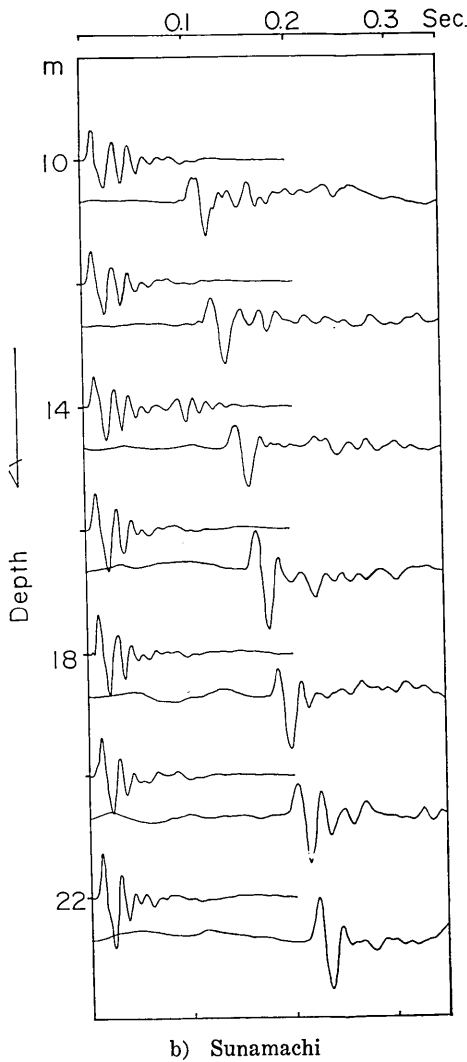


Fig. 3b, c and d. Sample seismograms of vertically travelling SH waves. Shorter ones are reference seismograms obtained at fixed position A.

in these strata were used in the present investigation. They are shown in Figs. 3a, 3b, 3c and 3d together with the reference seismograms (shorter ones in the figures) obtained at the position A fixed all through each experiment.

## 3. Analysis

As shown in Fig. 1, simultaneous observation was made at  $A$  and  $B$ . Let the Fourier transforms of the seismograms observed at  $A$  and  $B$  in  $i$ -th trial be

$$\begin{aligned} A_i(f) &= H_A(f) \cdot C_A(f) \cdot S_i(f), \\ B_i(f) &= H_{B_i}(f) \cdot C_B(f) \cdot S_i(f), \end{aligned}$$

where

|          |  |       |
|----------|--|-------|
| $f$      | Frequency  |       |
| $S(f)$   | Source spectrum  |       |
| $H_A(f)$ | Transfer function of medium between source point and $A$ |       |
| $H_B(f)$ | "  | $B$   |
| $C_A(f)$ | Frequency characteristics of apparatus used for $A$      |       |
| $C_B(f)$ | "  | $B$ . |

The transfer function  $H_{B_i}(f)$  is given by the following expression eliminating source spectrum

$$H_{B_i}(f) = \frac{B_i(f)}{A_i(f)} \cdot \frac{C_A(f) \cdot H_A(f)}{C_B(f)}.$$

Seismic waves in the lossy medium can be expressed as follows ;

$$F(f) = G \exp[-\{\alpha(f) + ik\}R],$$

where

- $G$  Geometrical factor
- $R$  Distance between the source and the seismometer
- $k$  Wave number.

Then, the attenuation coefficient  $\alpha(f)$  is given as follows

$$\begin{aligned} \alpha(f) &= - \frac{\log [G_i^{-1} H_{B_i}(f) / G_j^{-1} H_{B_j}(f)]}{R_i - R_j} \\ &= - \frac{\log [G_i^{-1} \{B_i(f) / A_i(f)\} / G_j^{-1} \{B_j(f) / A_j(f)\}]}{R_i - R_j}. \end{aligned}$$

After Onda and Komaki (1965), waves observed in the direction bisecting the source plate are the waves of SH type alone. Since the observations were made at sufficiently far distances from the source point the effect of plate length can be safely ignored. Accordingly, the spherical spreading of waves was assumed in computing the geometrical factor.

The thickness of constant velocity layer used in the analysis was not so thick. In such a case, as pointed out by McDonal et al (1958), reflected and refracted waves at the interfaces at various depths may interfere with the useful signals. Fortunately, the velocity contrast in our experimental site was not so remarkable and the interference was negligible although the reflected wavelets were detected in the case of Adachi. As can be seen in Fig. 3a, the reflected wavelets from the deep interface were distinguishable from the down-going wavelets. So we could analyse the useful signals without the fear of interference.

A hanning window was applied in the spectral analysis. The duration of window was 0.08 second, and the sampling interval was 1 or 2 millisecond.

#### 4. Results and Discussions

Fourier amplitudes of seismograms obtained at various depths were corrected by means of the geometrical factors. As an example, the case of Adachi is shown in Fig. 4. Figure 5 shows the relation between

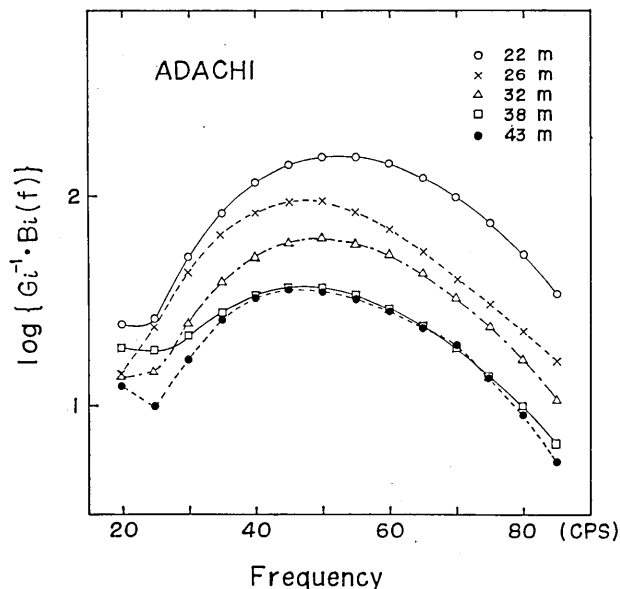


Fig. 4. An example of Fourier spectra corrected by the geometrical factor for spherical spreading (Adachi).

$\log \{G_i^{-1} B_i(f)\}$  and depth for various frequencies in the case of Adachi. The mean value and standard deviation for each frequency were calculated applying the regression line analysis. The relations between attenuation coefficients and frequencies are shown in Figs. 6a (Adachi),

6b (Sunamachi), 6c (Yukigaya) and 6d (Yayoi). The mean values and standard deviations are shown by circles and vertical bars, respectively. The attenuation coefficient in the Maxwell solid is almost independent of frequency and that in the Voigt solid is proportional to the square of frequency. Comparing this with our results, it was found that

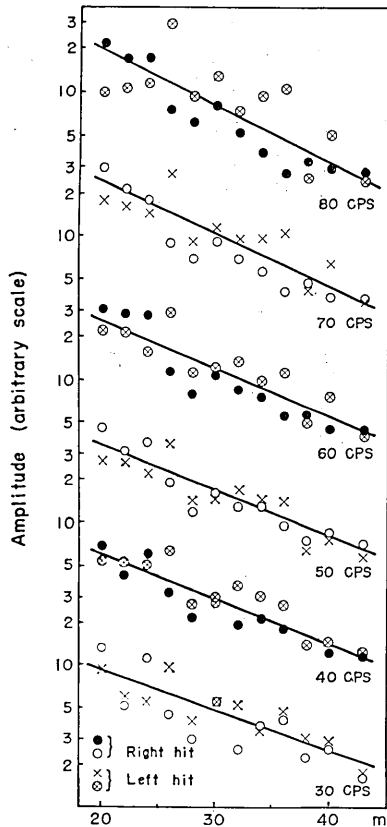


Fig. 5. Relation between  $\log\{G_i^{-1}H_{Bi}(f)\}$  and depth for various frequencies in the case of Adachi.

the attenuation coefficients agreed neither with the Maxwell model nor the Voigt model. If we assume that the attenuation of waves is due to the solid friction, attenuation coefficient is proportional to frequency. With this assumption in mind the straight lines were drawn as shown in Fig. 6a, 6b, 6c and 6d. These lines fitted better than those of the former cases. Figure 7 shows the phase velocity calculated from phase angles of Fourier transform, with respect to the frequency, in the case of Adachi. The regression line analysis was also applied to calculating the mean value (shown by circles) and standard deviation (shown by vertical bars) for each frequency. From the figure, it seems that the dispersion of SH waves is negligible, even if it does exist. As this result, it is concluded that it is hard to explain the loss mechanism by means of the

Maxwell model or the Voigt model.

Now we will discuss the loss mechanism in terms of  $Q$ -value. The  $Q$ -value can be expressed by the formula

$$Q = \frac{\pi f}{c \cdot \alpha(f)},$$

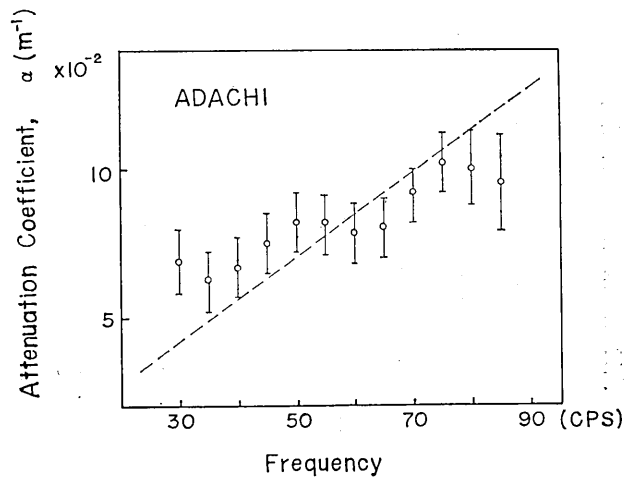
in which  $c$  is the phase velocity. The  $Q$ -values for various frequencies were obtained in the case of Adachi and are shown by circles in Fig. 8. As can be seen in the figure,  $Q$ -values scarcely depend on frequency. As a reference,  $Q$ -values were computed in the case of the Maxwell



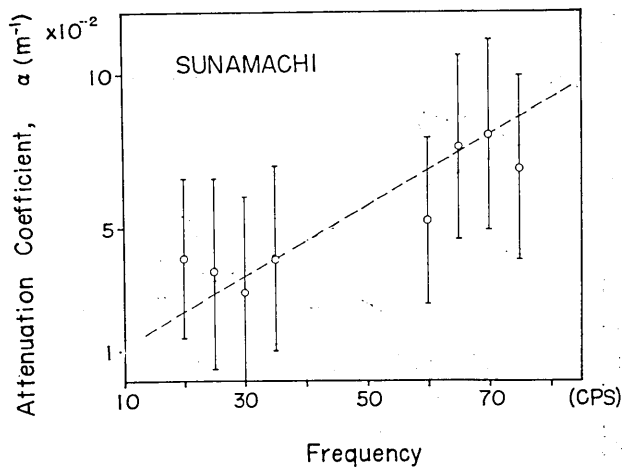
model and the Voigt model choosing the constants so that the values fit the observations at about 50 cps. They are also shown in Fig. 8.

Chae (1968) suggested the loss mechanism of snow and sand introducing the theory of linear viscoelasticity. The complex compliance is expressed as follows

$$J^*(i\omega) = J_\infty - \frac{i}{\omega\eta'} + \int_0^\infty \frac{D(\tau')}{1+i\omega\tau'} d\tau'$$



(a)

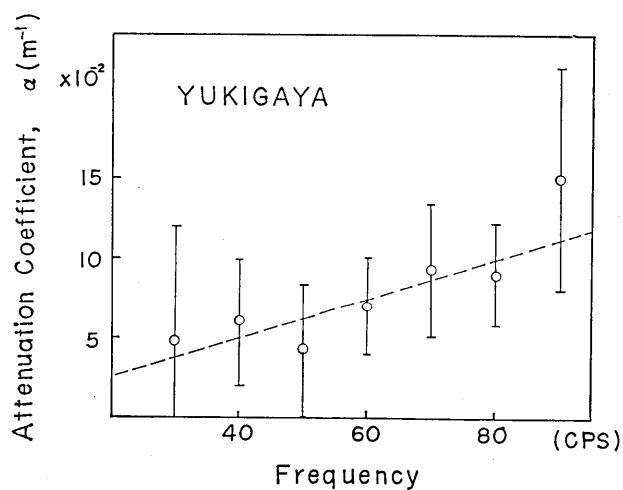


(b)

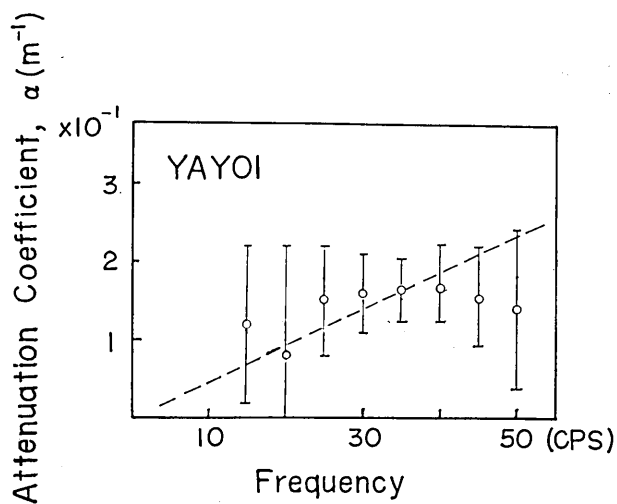
Fig. 6a, b. Attenuation coefficient vs. frequency. The mean values and the standard deviations are shown by circles and vertical bars, respectively.

in which  $J_\infty$  is compliance at infinitely large frequency,  $\eta'$  is viscosity,  $\tau'$  is retardation time,  $D(\tau')$  is the distribution function of retardation time. Chae assumed that

$$\left. \begin{aligned} J_\infty &= 0, & 1/\eta' &= 0, \\ D(\tau') &= \beta'/\tau' & \tau'_1 < \tau' < \infty \\ &= 0 & \tau' < \tau'_1. \end{aligned} \right\}$$



(c)



(d)

Fig. 6c, d. Attenuation coefficient vs. frequency. The mean values and the standard deviations are shown by circles and vertical bars, respectively.

Since the  $Q$ -value is expressed by the ratio of real to imaginary parts of complex compliance,  $Q$ -value vs. frequency for Chae's model is given as follows

$$Q = \frac{\log(1 + 1/\omega^2\tau_1'^2)}{2 \arctan(1/\omega\tau_1')} .$$

The broken line in Fig. 8 shows the value computed when  $\tau_1'$  equals to  $10^{-7}$  sec. by the above equation.

Meanwhile, complex rigidity which is the reciprocal of complex compliance, is expressed as follows

$$G^*(i\omega) = G_0 + i\omega\eta + i\omega \int_0^\infty \frac{F(\tau)\tau}{1 + i\omega\tau} d\tau ,$$

in which  $G_0$  is rigidity at zero frequency,  $\eta$  is viscosity,  $\tau$  is relaxation time,  $F(\tau)$  is the distribution function of relaxation time. Let us assume

$$\left. \begin{aligned} G_0 &= 0 , & \eta &= 0 , \\ F(\tau) &= \beta/\tau & \tau_1 < \tau < \tau_2 & \\ &= 0 & \text{otherwise} . & \end{aligned} \right\}$$

Under the above assumption

$$Q = \frac{1}{2} \cdot \frac{\log(1 + \omega^2\tau_2^2) - \log(1 + \omega^2\tau_1^2)}{\arctan(\omega\tau_2) - \arctan(\omega\tau_1)} .$$

An example of  $Q$ -value vs. frequency, when  $\tau_1=0$  and  $\tau_2=10^3$  sec., is shown by the thick solid line in Fig. 8. As can be seen in the figure, this model agreed well with the observed value. However, considering the accuracy of our observation, and since the frequency range in our observations was quite limited, no further detailed discussion will be made.

The  $Q$ -values, SH waves velocities and other properties of soils obtained at four sites are tabulated in Table 2. The  $Q$ -values given in the Table are the averaged values over the frequency measured.

Table 2.

| No. | Location  | S-wave velocity | $Q$ | Geology           |
|-----|-----------|-----------------|-----|-------------------|
| 1   | Adachi    | 260m/s          | 8   | Diluvial sand     |
| 2   | Sunamachi | 102m/s          | 20  | Alluvial silt     |
| 3   | Yukiga    | 420m/s          | 6.5 | Tertiary mudstone |
| 4   | Yayoi     | 150m/s (mean)   | 5   | Kwanto loam       |

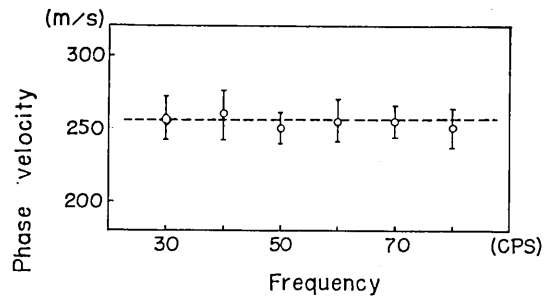


Fig. 7. Phase velocity vs. frequency (Adachi). The mean values and the standard deviations are shown by circles and vertical bars, respectively.

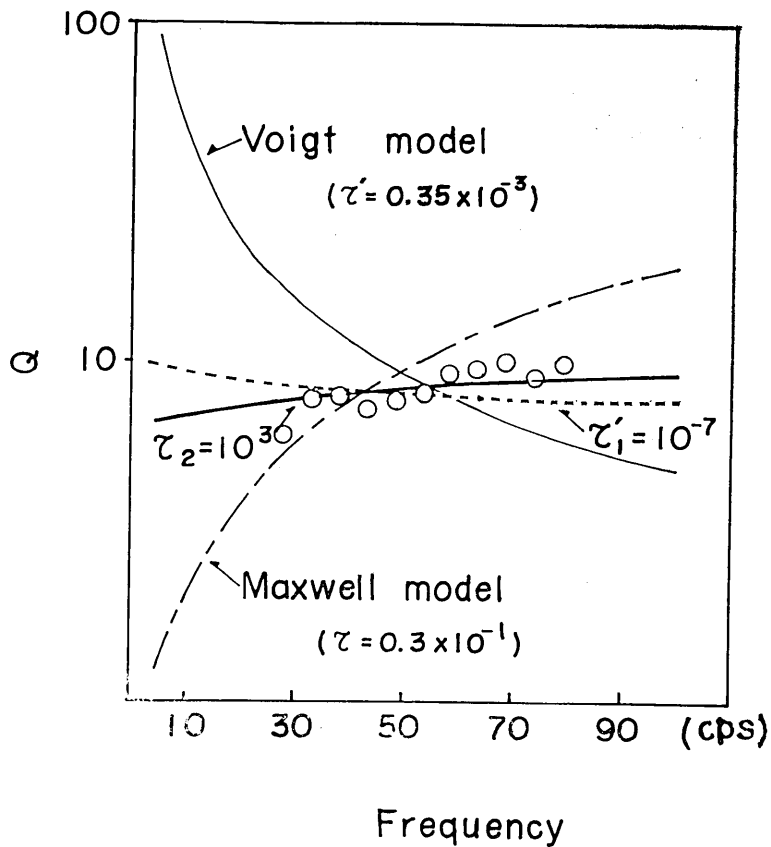


Fig. 8. Relation between  $Q$  and frequency. The observed values are shown by circles. Thin solid and part of a dotted line show the case of the Voigt model ( $\tau' = 0.35 \times 10^{-3}$  sec.) and the Maxwell model ( $\tau = 0.3 \times 10^{-1}$  sec.), respectively. The broken and thick solid lines show the Chae's model ( $\tau_1' = 10^{-7}$  sec.) and the model assumed in this paper ( $\tau_1 = 0$ ,  $\tau_2 = 10^3$  sec.), respectively.

## Acknowledgement

The authors express their hearty thanks to Professor H. Kawasumi for his valuable suggestion extended to them. Their thanks are also due to Dr. I. Onda and Dr. Y. Ohta for their discussions and to Mr. M. Yanagisawa and Mrs. S. Miyagi for their help in conducting the experiments.

## References

- BORN, W.T., 1941, The attenuation constant of earth materials, *Geophysics*, **6**, 132-148.
- CHAE, Y.S., 1968, Viscoelastic properties of snow and sand, *J. Engineering Mechanics Division*, ASCE, **94**, 1379-1394.
- COLLINS, F. and C. C. LEE, 1956, Seismic wave attenuation characteristics from pulse experiments, *Geophysics*, **21**, 16-39.
- FUTTERMAN, W. I., 1962, Dispersive body waves, *J. Geophys. Res.*, **67**, 5279-5291.
- HIRONO, T., 1935a, On the viscoelastic waves (I), *J. Met. Soc. Japan*, [ii], **13**, 413-424, (in Japanese).
- HIRONO, T., 1935b, On the viscoelastic waves (II), *J. Met. Soc. Japan*, [ii], **13**, 512-520, (in Japanese).
- HIRONO, T., 1941, On the viscoelastic waves (III), *Quart. J. Seismol.*, **11**, 337-348, (in Japanese).
- HORTON, C.W., 1959, A loss mechanism for Pierre shale, *Geophysics*, **24**, 667-680.
- IIDA, K., 1934, Experiments on the visco-elastic properties of pitch-like materials. (I), *Bull. Earthq. Res. Inst.*, **13**, 198-212.
- IIDA, K., 1935, Experiments on the visco-elastic properties of pitch-like materials. (II), *Bull. Earthq. Res. Inst.*, **13**, 433-156.
- IIDA, K., 1938a, Relation between the normal-tangential viscosity ratio and Poisson's elasticity ratio in certain soils, *Bull. Earthq. Res. Inst.*, **16**, 391-406.
- IIDA, K., 1938b, Elastic and viscous properties of a certain kind of rock, *Bull. Earthq. Res. Inst.*, **17**, 59-78.
- IIDA, K., 1938c, Determination of Young's modulus and the solid viscosity coefficients of rocks by the vibration method, *Bull. Earthq. Res. Inst.*, **17**, 79-92.
- ISHIMOTO, M. and K. IIDA, 1936a, Determination of elastic constants of soil by means of vibration method, Part I, Young's modulus, *Bull. Earthq. Res. Inst.*, **14**, 632-657.
- ISHIMOTO, M. and K. IIDA, 1936b, Determination of elastic constants of soil by means of vibration method, Part II, Modulus of rigidity and Poisson's ratio, *Bull. Earthq. Res. Inst.*, **15**, 67-88.
- KELVIN, LORD, 1878, Elasticity, in *Encyclopedia Britannica*, ninth edition.
- KNOPOFF, I., 1956, The seismic pulse in materials possessing soil friction, 1, Plane waves, *Bull. Seismol. Soc. Am.*, **46**, 175-183.
- KNOPOFF, I. and G. J. F. MACDONALD, 1958, Attenuation of small amplitude stress waves in solids, *Rev. Mod. Phys.*, **30**, 1178-1192.
- KUBOTERA, A., 1952, Rheological properties of earth's crust and alluvial layers in relation to propagation of seismic waves, *J. Phys. Earth*, **1**, 25-34.
- LOMNITZ, C., 1957, Linear dissipation in solids, *J. Appl. Phys.*, **28**, 201-205.
- LOMNITZ, C., 1962, Application of the logarithmic creep law to stress wave attenuation in the solid earth, *J. Geophys. Res.*, **67**, 365-367.
- MAXWELL, J. C., 1867, On the dynamical theory of gases, *Phil. Trans. Roy. Soc. London*, **157**, 49-88.

- McDONAL, F. J., F. A. ANGONA, R. L. MILLS, R. L. SENGBUSH, R. G. VAN NOSTRAND and J. E. WHITE, 1958, Attenuation of shear and compressional waves in Pierre shale, *Geophysics*, **23**, 421-439.
- MEYER, O. E., 1874a, Zur Theorie der inner Reibung, *J. Reine Angew. Math.*, **58**, 130-135.
- MEYER, O. E., 1874b, Theorie der elastischen Nachwirkung, *Ann. Phys.*, **227**, 108-119.
- MIYABE, N. and T. OOI, 1948, On longitudinal vibration tests, *Zisin (Bull. Seismol. Soc. Japan)*, [ii], **1**, 2-3, (in Japanese).
- ONDA, I. and S. Komaki, 1965, Waves generated from a linear horizontal traction with finite source length on the surface of a semi-infinite elastic medium, with special remarks on the theory of shear wave generator, *Bull. Earthq. Res. Inst.*, **46**, 1-23.
- RICKER, N., 1941, A note on the determination of the viscosity of shale from the measurement of wavelength breadth, *Geophysics*, **6**, 254-258.
- SHIMA, E., Y. OHTA, M. YANAGISAWA, K. KUDO and H. KAWASUMI, 1968, S wave velocities of subsoil layers in Tokyo. 3, *Bull. Earthq. Res. Inst.*, **46**, 1301-1312, (in Japanese).
- STRICK, E., 1967, The determination of Q, dynamic viscosity and transient creep from wave propagation measurements, *Geophys. J. Roy. Astro. Soc.*, **13**, 197-218.
- TULLOS, F. and A. REID, 1969, Seismic attenuation of Gulf Coast sediments, *Geophysics*, **34**, 516-528.
- VOIGT, W., 1892, Über Innere Reibung fester Körper, Insbesondere der Metalle, *Ann. Phys.*, **47**, 671-693.
- WUENSCHEL, P. C., 1965, Dispersive body waves—An experimental study, *Geophysics*, **30**, 539-551.

## 10. 軟弱な地層における S 波の減衰

地震研究所 { 工 藤 一 嘉  
                  嶋 悦 三

ごく最近に到るまで、現場における S 波の発生は困難であるとされていたため、S 波の減衰に関する研究は極めて少ない。地震波の減衰機構は、動的な応力・歪の関係と対応するから、物質の物理的性質を知る上で、詳しく調べておく必要がある。また応用の見地から、構築物が軟弱な地盤の上に建てられる場合が多いので、地震時における地盤の挙動を熟知する必要があるが、そのためにも軟弱な地層での減衰機構に関する知識が不可欠である。

今回、板叩き法により S 波を発生させ、抗井法で得られた記録をフーリエ解析し、S 波の減衰を調べた。その結果、地質により多少異なるが、調べた周波数範囲内では、減衰係数が周波数に比例する傾向が強く、また位相速度の分散性も、非常に小さい。したがって、Q の周波数依存性は、あるとしても非常に小さいことが解つた。この結果を単純な Maxwell 模型や Voigt 模型で説明することは難しい。しかしながら、必ずしもこの結果を固体摩擦で説明しなくとも、適当な仮定を設けることにより、線型粘弾性理論で説明出来る可能性のあることを示しておいた。

このような点をさらに解明するためには、測定周波数範囲を広げなければならない。測定の精度の向上とあわせ、上記の努力を続けるつもりである。